JOURNAL OF AIRCRAFT
Vol. 42, No. 2, March–April 2005

Efficient Optimization Design Method Using Kriging Model

Shinkyu Jeong,* Mitsuhiro Murayama,† and Kazuomi Yamamoto‡
Japan Aerospace Exploration Agency, Tokyo 182-8522, Japan

The kriging-based genetic algorithm is applied to aerodynamic design problems. The kriging model is a response surface model that represents a relationship between objective function (output) and design variables (input) using a stochastic process. The kriging model drastically reduces the computational time required for objective function evaluation in the optimization (optimum searching) process. Expected improvement is used as a criterion to select additional sample points. This makes it possible not only to improve the accuracy of the response surface, but also to explore the global optimum efficiently. The functional analysis of variance (ANOVA) is conducted to evaluate the influence of each design variable and their interactions to the objective function. Based on the result of the functional ANOVA, designers can reduce the number of design variables by eliminating those that have small effect on the objective function. The present method is applied to a two-dimensional airfoil design and the prediction of flap's position in a multi-element airfoil, where the lift-to-drag ratio (*L/D*) is maximized.

Nomenclature

A	=	cross-sectional area of airfoil
$d(\cdot, \cdot)$	=	distance function between two points
$E[I(\cdot)]$	=	expected improvement
L/D	=	lift-to-drag ratio
$\boldsymbol{R}$	=	correlation matrix for kriging model
$\boldsymbol{r}'$	=	vector of correlation values for kriging model
$s^2(\cdot)$	=	mean squared error of the predictor
x	=	scalar component of $\boldsymbol{x}$
$\boldsymbol{x}$	=	vector denoting position in the design space
$\boldsymbol{y}$	=	vector of response data
$y(\cdot)$	=	unknown function
$\hat{y}(\cdot)$	=	estimated value of $y(\cdot)$
$Z(\cdot)$	=	deviation from constant model
β	=	constant global model of kriging model
$\hat{\beta}$	=	estimated value of β
$\boldsymbol{\theta}$	=	vector of correlation parameters for kriging model
$\hat{\mu}_{\text{total}}$	=	total mean of model
$\hat{\sigma}^2$	=	estimated sample variance
$\hat{\sigma}^2_{\text{total}}$	=	total variance of model
Φ	=	standard normal distribution
ϕ	=	standard normal density

Introduction

WITH the growth in computing power of current computers and the advances in computational techniques, today computational fluid dynamics (CFD) has become an invaluable tool for aerodynamic optimization design. However, in the process of optimization design, the number of objective function evaluations using high-fidelity CFD analysis solvers, is severely limited by time and cost, even with current supercomputers.

One alternative is to construct a simple approximate model of the complicated CFD analysis solver. The approximate model expresses the relationship between the objective function (output) and the design variables (input) with a simple equation. This model requires very little time to evaluate objective function. It enables us to save a lot of computation time and to explore a wider design space.

The most widely used approximation model is the polynomial-based model[1,2] because of its simplicity and ease of use. However, this model is not suitable for representing multimodality and nonlinearity of the aerodynamic problem.

Recently, the kriging model,[3,4] developed for use in the fields of spatial statistics and geostatistics, has gained popularity for aerodynamic design. This model predicts the value of the unknown point using stochastic processes. Sample points are interpolated with the Gaussian random function to estimate the trend of the stochastic processes. The model has sufficient flexibility to represent the nonlinear and multimodal functions at the expense of computation time. However, the computation time to construct the kriging model is still short compared to that of direct CFD analysis.

In this study, genetic algorithms (GAs) are adopted as the searching algorithm. GAs are based on the mechanism of natural selection and genes. GAs are very attractive for engineering problems where discontinuities and multimodalities may exist because GAs do not utilize derivative information. Another merit of GAs is that they search the optimum point from a population of points, not a single point. This feature is very promising for multi-objective problems.

However, GAs require many objective function evaluations, which may be impractical if we rely solely on the time-consuming high-fidelity CFD analysis solver. Here, the time-consuming CFD analysis solver in the objective function evaluation process of GA is replaced with the kriging model. Note, however, that it is possible to miss the global optimum in the searching space if we rely only on the prediction value of the kriging model because the model includes uncertainty at the prediction point. For robust exploration of the global optimum point, both the prediction value and its uncertainty should be considered at the same time. This concept is expressed in the criterion expected improvement (EI). EI indicates the probability of a point being optimum in the design space. By the selection of the best EI point as the additional sample point, improvement of the model and robust exploration of the global optimum can be achieved at the same time.

Current optimization design problems treat a large number of design variables, sometimes on the order of several hundreds. In this study, a variance decomposition of the model, using a functional analysis of variance (ANOVA),[5,6] is employed to evaluate the effect of each variable and its interactions with the objective function. Based on these results, a design variable that does not have significant influence on the objective function can be eliminated.

Presented as Paper 2004-0118 at the 42nd AIAA Aerospace Sciences Meeting and Exhibit Reno, NV, 5–8 January 2004; received 10 November 2003; revision received 25 February 2004; accepted for publication 12 April 2004.

*Invited Scientist, Information Technology Center, Institute of Space Technology and Aeronautics, Chofu; jeong@chofu.jaxa.jp. Associate Member AIAA.

†Scientist, Information Technology Center, Institute of Space Technology and Aeronautics, Chofu; murayama@chofu.jaxa.jp. Member AIAA.

‡Senior Researcher, Information Technology Center, Institute of Space Technology and Aeronautics, Chofu; kazuomi@chofu.jaxa.jp. Member AIAA.

Kriging Model

The present kriging model expresses the unknown function $y(\boldsymbol{x})$ as

$$y(\boldsymbol{x}) = \beta + Z(\boldsymbol{x}) \tag{1}$$

where $\boldsymbol{x}$ is an m-dimensional vector (m design variables), β is a constant global model, and $Z(\boldsymbol{x})$ represents a local deviation from the global model. In the model, the local deviation at an unknown point $\boldsymbol{x}$ is expressed using stochastic processes. The sample points are interpolated with the Gaussian random function as the correlation function to estimate the trend of the stochastic processes. The correlation between $Z(\boldsymbol{x}^i)$ and $Z(\boldsymbol{x}^j)$ is strongly related to the distance between the two corresponding points $\boldsymbol{x}^i$ and $\boldsymbol{x}^j$. In the kriging model, a special weighted distance is used instead of the Euclidean distance, as follows:

$$d(\boldsymbol{x}^i, \boldsymbol{x}^j) = \sum_{k=1}^{m} \theta_k \left| x_k^i - x_k^j \right|^2 \tag{2}$$

where θ_k $(0 \le \theta_k \le \infty)$ is the kth element of the correlation vector parameter $\boldsymbol{\theta}$. When the specially weighted distance and the Gaussian random function are used, the correlation between the point $\boldsymbol{x}^i$ and $\boldsymbol{x}^j$ is defined as

$$\text{corr}\lfloor Z(\boldsymbol{x}^i), Z(\boldsymbol{x}^j)\rfloor = \exp\lfloor -d(\boldsymbol{x}^i, \boldsymbol{x}^j)\rfloor \tag{3}$$

The kriging predictor[7] is

$$\hat{y}(\boldsymbol{x}) = \hat{\beta} + \boldsymbol{r}'\boldsymbol{R}^{-1}(\boldsymbol{y} - \mathbf{1}\hat{\beta}) \tag{4}$$

where $\hat{\beta}$ is the estimated value of β, $\boldsymbol{R}$ is the $n \times n$ matrix whose (i, j) entry is corr $\lfloor Z(\boldsymbol{x}^i), Z(\boldsymbol{x}^j)\rfloor$, $\boldsymbol{r}$ is vector whose ith element is

$$r_i(\boldsymbol{x}) \equiv \text{corr}\lfloor Z(\boldsymbol{x}), Z(\boldsymbol{x}^i)\rfloor \tag{5}$$

and $\boldsymbol{y} = [y(x^1), \ldots, y(x^n)]$.

The unknown parameter to be estimated for constructing the kriging model is $\boldsymbol{\theta}$. This parameter can be estimated by maximizing the following likelihood function:

$$\ell_n(\hat{\beta}, \hat{\sigma}^2, \boldsymbol{\theta}) = -(n/2)\,\ell_n(2\pi) - \tfrac{1}{2}\ell_n(|\boldsymbol{R}|)$$

$$-(n/2)\ell_n(\hat{\sigma}^2) - (1/2\hat{\sigma}^2)(\boldsymbol{y} - \mathbf{1}\hat{\beta})'\boldsymbol{R}^{-1}(\boldsymbol{y} - \mathbf{1}\hat{\beta}) \tag{6}$$

where $\mathbf{1}$ is an m-dimensional unit vector.

Maximizing the likelihood function is an m-dimensional unconstrained nonlinear optimization problem. In this paper, the alternative method[8] is adopted to solve this problem.

For a given $\boldsymbol{\theta}$, here $\hat{\beta}$ and $\hat{\sigma}^2$ can be defined as

$$\hat{\beta} = (\mathbf{1}'\boldsymbol{R}^{-1}\boldsymbol{y})/(\mathbf{1}'\boldsymbol{R}^{-1}\mathbf{1}) \tag{7}$$

$$\hat{\sigma}^2 = (\boldsymbol{y} - \mathbf{1}\hat{\beta})'\boldsymbol{R}^{-1}(\boldsymbol{y} - \mathbf{1}\hat{\beta})/n \tag{8}$$

Next, vector $\boldsymbol{\theta}$ is updated by using

$$\boldsymbol{\theta}^{\text{new}} = \boldsymbol{\theta}^{\text{old}} + \boldsymbol{B}^{-1}\frac{\partial \ell_n}{\partial \boldsymbol{\theta}} \tag{9}$$

where

$$\frac{\partial \ell_n}{\partial \theta_k} = -\frac{1}{2}\text{tr}\left\{\frac{1}{\boldsymbol{R}}\frac{\partial \boldsymbol{R}}{\partial \theta_k}\right\} - \frac{1}{2\sigma^2}(\boldsymbol{y} - \mathbf{1}\beta)'\frac{1}{\boldsymbol{R}}\frac{\partial \boldsymbol{R}}{\partial \theta_k}\frac{1}{\boldsymbol{R}}(\boldsymbol{y} - \mathbf{1}\beta) \tag{10}$$

and the (i, j)th element of matrix $\boldsymbol{B}$ is $\frac{1}{2}t_{ij}$ with

$$t_{ij} = \text{tr}\left(\boldsymbol{R}^{-1}\frac{\partial \boldsymbol{R}}{\partial \theta_i}\boldsymbol{R}^{-1}\frac{\partial \boldsymbol{R}}{\partial \theta_j}\right) \tag{11}$$

For this updated $\boldsymbol{\theta}^{\text{new}}$, the new values of $\hat{\beta}$ and $\hat{\sigma}^2$ can be calculated using Eqs. (7) and (8). This routine is iterated until the function ℓ_n converges to a maximum value.

The accuracy of the prediction value largely depends on the distance from sample points. Intuitively speaking, the closer point $\boldsymbol{x}$ to the sample point, the more accurate is the prediction $\hat{y}(\boldsymbol{x})$. This intuition is expressed as

$$s^2(\boldsymbol{x}) = \hat{\sigma}^2\left[1 - \boldsymbol{r}'\boldsymbol{R}^{-1}\boldsymbol{r} + \frac{(1 - \mathbf{1}\boldsymbol{R}^{-1}\boldsymbol{r})^2}{\mathbf{1}'\boldsymbol{R}^{-1}\mathbf{1}}\right] \tag{12}$$

where $s^2(\boldsymbol{x})$ is the mean squared error of the predictor and it indicates the uncertainty at the estimation point. The root mean squared error (RSME) is expressed as $s = \sqrt{s^2(\boldsymbol{x})}$.

GAs as Optimizers

GAs[9] are searching mechanisms based on natural selection and genetics. GAs use the objective function value itself, not its derivative information. This feature makes GAs robust and attractive for aerodynamic design problems where nonlinearity, multimodality, and discontinuities may exist. Another merit of GAs is that they search the optimum point from a population of points, not a single point. This makes GAs a promising method for multi-objective (MO) problems. The population of points can represent Pareto optimal set of MO problems.[10] The definition of Pareto optimality is as follows.

Suppose $X_1 = (x_1, y_1)$ and $X_2 = (x_2, y_2)$ are in the population and $F = (f_1, f_2)$ is the set of objective functions to be maximized.

1) X_1 is said to be dominated by X_2 if $F(X_1)$ is partially less than $F(X_2)$, that is, $f_1(X_1) \le f_1(X_1) \bigcap f_2(X_1) \le f_2(X_2)$ and $F(X_1) \ne F(X_2)$.

2) X_1 is said to be nondominated if there does not exist X_2 in the population that dominates X_1. In Fig. 1, black circled are the Pareto solutions. Each point in the Pareto set is optimal in the sense that no improvement can be achieved in any objective function without degradation in the others.

The general procedure of GAs is shown in Fig. 2: 1) creation of initial population, 2) evaluation of fitness (objective) function, 3) selection of parents according to the rank (fitness), 4) crossover and mutation, and 5) check of the convergence. If not converged, return to the process step 2.

Exploration of the Global Optimization and Improvement of the Model

Once the approximation model is constructed, the optimum point can be explored using an arbitrary optimizer on the model. However, it is possible to miss the global optimum because the approximation model includes uncertainty at the predicted point.

In Fig. 3, the solid line is the real shape of objective function. Eight points are selected to construct the kriging model, which is shown as dotted line. The minimum point on the kriging model is located near $x = 9$, whereas, the real global minimum of the objective function is situated near $x = 4$. Searching for the global minimum using the present kriging model will not result in the real global minimum

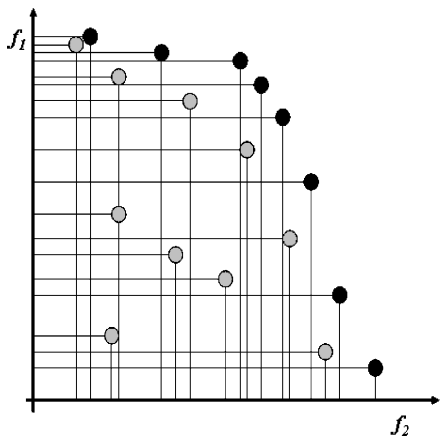

Fig. 1 Pareto set of a MO problem.

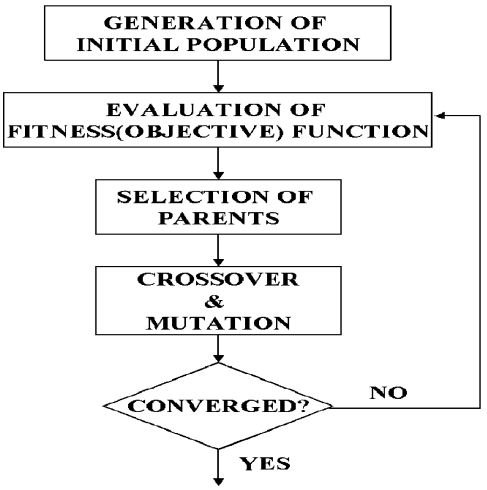

Fig. 2 Flow chart of GAs.

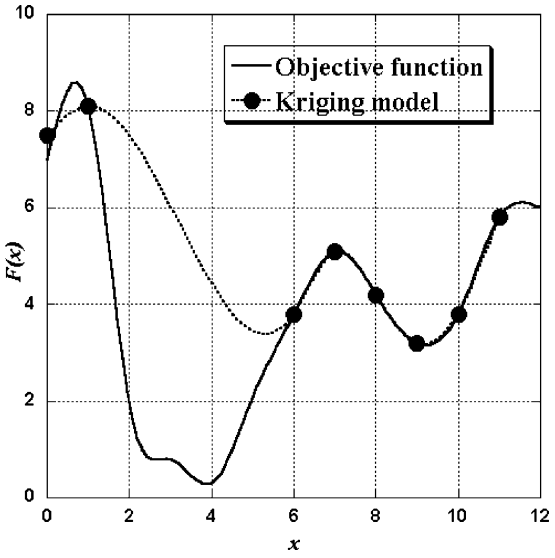

Fig. 3 Objective function and kriging model.

near $x = 4$. For a robust search of the global optimum, both the predicted value by the kriging model and its uncertainty should be considered at the same time.

Figure 4 shows the predicted value and the standard error of the kriging model. Around $x = 9.5$, the standard error of the kriging model is very small because there are many sample points around this point. Thus, the confidence interval is very short, as shown in Fig. 4.

On the other hand, the standard error is very large around $x = 3.5$ because of the lack of sample points around there. Thus, the confidence interval at this point is very wide. The minimum inside this interval is less than the present minimum point on the kriging model. This point has a somewhat large probability to become the global minimum.

This concept is expressed in the criterion of EI.[11] The EI of minimization problem can be calculated as

$$E[I(\boldsymbol{x})] = (f_{\min} - \hat{y})\Phi[(f_{\min} - \hat{y})/s] + s\phi[(f_{\min} - \hat{\boldsymbol{y}})/s] \quad (13)$$

where $f_{\min}$ is the minimum value among n sampled values. Φ and ϕ are the standard distribution and normal density, respectively. By selecting the maximum EI point as additional sample point, robust exploration of the global optimum and improvement of the model can be achieved simultaneously.

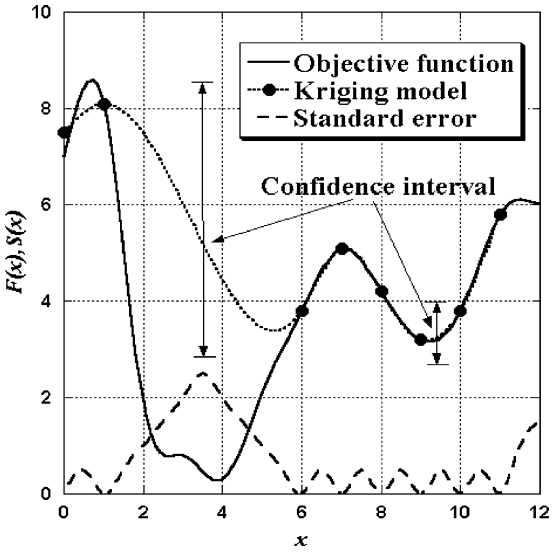

Fig. 4 Predicted value and the standard error of kriging model.

Visualization of Model

One of the advantages of using approximation model is that it shows the relationship between the objective function and design variables. This relationship is very helpful to identify how much influence each design variable has on the objective function. Based on the result, the designer can eliminate the design variables that do not have significant effect on objective function. To evaluate the effect of each design variable, the total variance of the model is decomposed into that of each design variable and their interactions. It is called the functional ANOVA. The decomposition is accomplished by integrating variables out of the model $\hat{y}$. The total mean $\hat{\mu}_{\text{total}}$ and variance $\hat{\sigma}^2_{\text{total}}$ of model $\hat{y}$ are as follows:

$$\hat{\mu}_{\text{total}} \equiv \int \cdots \int \hat{y}(x_1, \ldots, x_n)\, \mathrm{d}x_1 \ldots \mathrm{d}x_n \quad (14)$$

$$\hat{\sigma}^2_{\text{total}} \equiv \int \cdots \int [\hat{y}(x_1, \ldots, x_n) - \hat{\mu}]^2\, \mathrm{d}x_1 \ldots \mathrm{d}x_n \quad (15)$$

The main effect of variable x_i is

$$\hat{\mu}_i(x_i) \equiv \int \cdots \int \hat{y}(x_1, \ldots, x_n)\, \mathrm{d}x_1 \ldots \mathrm{d}x_{i-1}\, \mathrm{d}x_{i+1} \ldots, \mathrm{d}x_n - \hat{\mu} \quad (16)$$

The two-way interaction effect of variables x_i and x_j is

$$\hat{\mu}_{i,j}(x_{i,j}) \equiv \int \cdots \int \hat{y}(x_1, \ldots, x_n)\, \mathrm{d}x_1\, \mathrm{d}x_{i-1}\, \mathrm{d}x_{i+1} \ldots \mathrm{d}x_{j-1}\, \mathrm{d}x_{j+1} \ldots \mathrm{d}x_n - \hat{\mu}_i(x_i) - \hat{\mu}_j(x_j) - \hat{\mu} \quad (17)$$

where $\hat{\mu}_i(x_i)$ and $\hat{\mu}_{i,j}(x_i, x_j)$ quantify the effect of variable x_i and interaction effect of x_i and x_j on the objective function.

The variance due to the design variable x_i is

$$\int [\hat{\mu}_i(x_i)]^2\, \mathrm{d}x_i \quad (18)$$

The proportion of the variance due to design variable x_i to total variance of model can be expressed by dividing Eq. (18) by Eq. (15),

$$\frac{\int [\hat{\mu}_i(x_i)]^2\, \mathrm{d}x_i}{\int \cdots \int [\hat{y}(x_1, \ldots, x_n) - \hat{\mu}]^2\, \mathrm{d}x_1 \ldots \mathrm{d}x_n} \quad (19)$$

This value indicates the sensitivity of the objective function to the variation of the design variables and their interactions.

Results

In this study, the kriging-based GA was applied to a two-dimensional airfoil design and the optimization of a flap's position in a multi-element airfoil to maximize the lift-to-drag ratio L/D.

Airfoil Design

The first design problem is to maximize L/D of an airfoil at the condition of Mach = 2.0 and an angle of attack (AOA) = 2.0 deg, under the constraint of maintaining the cross-sectional area of the airfoil to the same level of the Royal Aircraft Establishment RAE2822 airfoil.

Definition of Airfoil Geometry and Design Variables

The geometry was parameterized using the PARSEC airfoil[12] definition. This parameterization technique was developed to keep the number of design variable as low as possible while controlling important transonic aerodynamic features effectively. Figure 5 shows 11 basic parameters for PARSEC airfoil: 1) leading edge radius r_{LE}, 2) trailing-edge coordinate Z_{TE}, 3) trailing-edge direction α_{TE}, 4) trailing-edge wedge angle β_{TE}, 5) crest of upper surface's X coordinateX_{up}, 6) crest of upper surface's Z coordinate Z_{up}, 7) curvature at the crest of upper surface $Z_{XX\mathrm{up}}$, 8) crest of lower surface's X coordinate X_{lo}, 9) crest of lower surface's Z coordinate Z_{lo}, 10) curvature at the crest of lower surface $Z_{XX\mathrm{lo}}$, and 11) trailing-edge thickness ΔZ_{TE}.

In this study, only sharp trailing-edge airfoil was considered, therefore, ΔZ_{TE} was set to zero. A total of 10 design variables were used to define the geometry of airfoil.

Design Space and Selection of Sample Points

The upper and lower bound of each parameter was determined to avoid unrealistic airfoil geometry, such as a fish-tailed airfoil. The parameter ranges of design space are shown in Table 1.

The number of sample points and their distribution is very important to obtain an accurate kriging model. A sufficient number of sample points should be spread over the design space uniformly. In this study, the sample points were selected by using the orthogonal arrays (OAs).[13] OAs have the beneficial property of distributing points in multidimensional design space uniformly. Important parameters of OAs are strength and level. If the OAs has strength k and level l, all projections to k dimension are uniformly distributed. The OAs used in this investigation has strength 2 and level 5 with 50 sample points. It may seem that the number of sample points is not sufficient to obtain the desirable accuracy of the present kriging model. However, additional sample points will be added later

Table 1 Parameter ranges of design space

Parameter	Lower bound	Upper bound
r_{LE}	0.005	0.06
X_{up}	0.35	0.50
Z_{up}	0.05	0.15
X_{lo}	0.35	0.50
Z_{lo}	0.12	−0.04
$Z_{XX\mathrm{up}}$	−1.0	−0.4
$Z_{XX\mathrm{lo}}$	0.3	1.0
Z_{TE}	−0.02	0.02
α_{TE}, deg	−8	−3
β_{TE}, deg	4	8

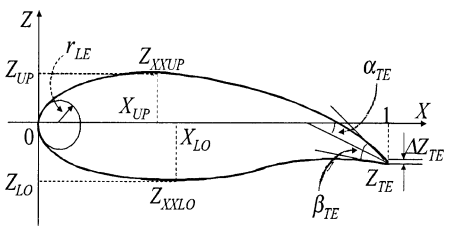

Fig. 5 PARSEC airfoil and its parameters.

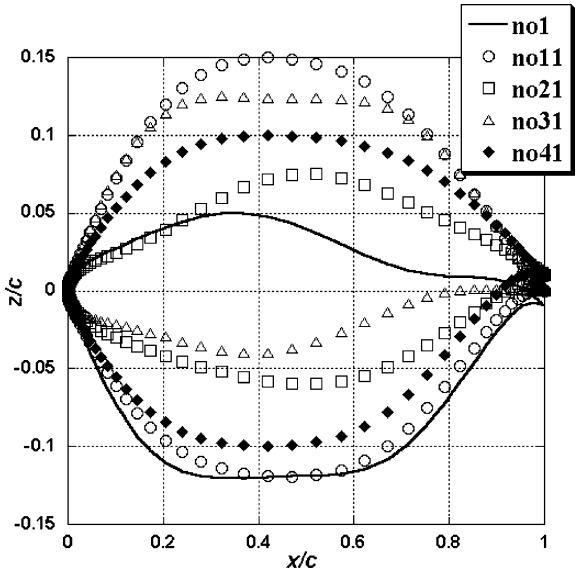

Fig. 6 Geometry of a number of sample airfoils.

in the region where the accuracy is not good enough, based on the EI evaluation. Figure 6 shows the geometry of a number of sample airfoils.

Genetic Algorithm with the Kriging Model

The performance of 50 sample airfoils was evaluated using a Navier–Stokes code. This code utilized a total variation diminishing (TVD) upwind scheme for spatial discretization of convective terms and a lower–upper symmetric Gauss–Seidel (LU-SGS) method (see Ref. 14) for time integration. A kriging model was then constructed based on the sample data, and the model was used for the objective function evaluation in the optimization process of the GA. However, as already discussed, if GA searches the maximum L/D point based only on the predicted value by kriging model, it may miss the global maximum point because the model has some uncertainty at the predicted point. In this study, the objective function L/D was transformed to the corresponding EI to find the global optimum point robustly. The design constraint was then treated as the other objective function of the optimization problem.

Thus, the single objective problem, the maximization of L/D, is changed to the MO problem, the maximization of both EI and area ratio. The objective functions are expressed as follows:

$$E[I(\boldsymbol{x})] = (\hat{y} - L/D_{\max})\Phi[(\hat{y} - L/D_{\max})/s] + s\phi[(\hat{y} - L/D_{\max})/s] \tag{20}$$

$$\text{area ratio} = 1. - \text{abs}(A - A_{\mathrm{RAE2822}})/A_{\mathrm{RAE2822}} \tag{21}$$

A_{RAE2822} is the cross-section area of an RAE2822 airfoil.

This MO problem was solved by MO GA (MOGA). The numbers of both the population and generations are 100. The Pareto set obtained by MOGA is shown in the Fig. 7.

Among the Pareto solutions, the airfoil that shows the highest L/D performance was selected as an additional sample. Then, the performance of the airfoil was evaluated by the Navier–Stokes code, and the kriging model was updated with 51 sample data. This routine was iterated until L/D was not improved any more. After five additional sample airfoil selections, there was no L/D improvement. The geometry and pressure distribution of the designed airfoil are shown in Fig. 8. The L/D and the cross-sectional area of the designed airfoil are compared with those of RAE2822 in Table 2. L/D has been improved within the design constraint.

Functional ANOVA

To estimate the main and the two-way interactions effect of design variables, the total variance of the model was decomposed into that of each design variable and their interactions. Figure 9 shows the

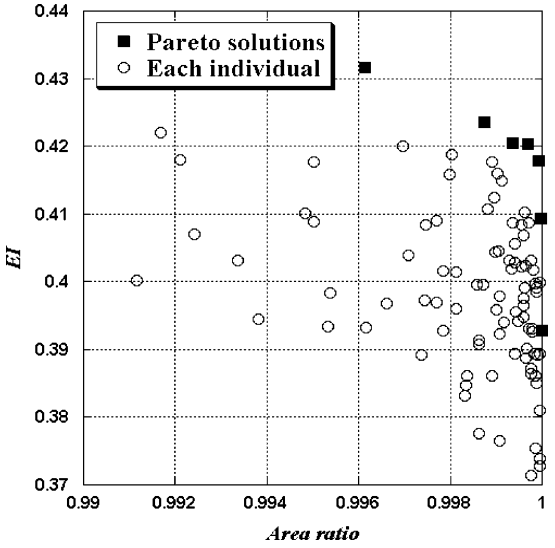

Fig. 7 Pareto solutions.

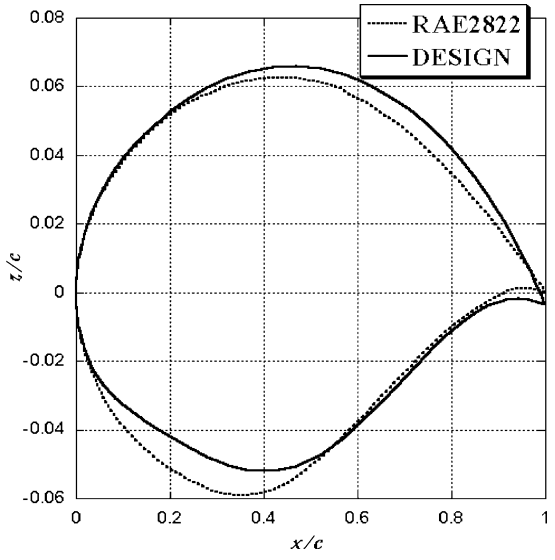

a)

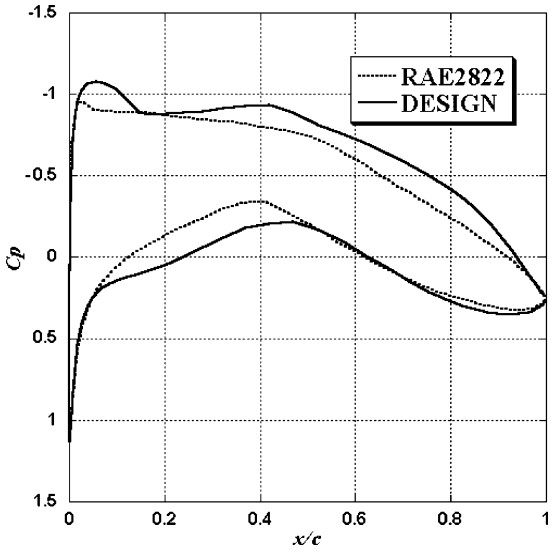

b)

Fig. 8 Comparisons of airfoils: a) geometry and b) pressure distribution.

Table 2 Comparison of *L/D* and cross-sectional area of airfoils

Airfoil	L/D	Area of cross section
RAE2822	58.0178	0.07777
Design	60.7546	0.07864

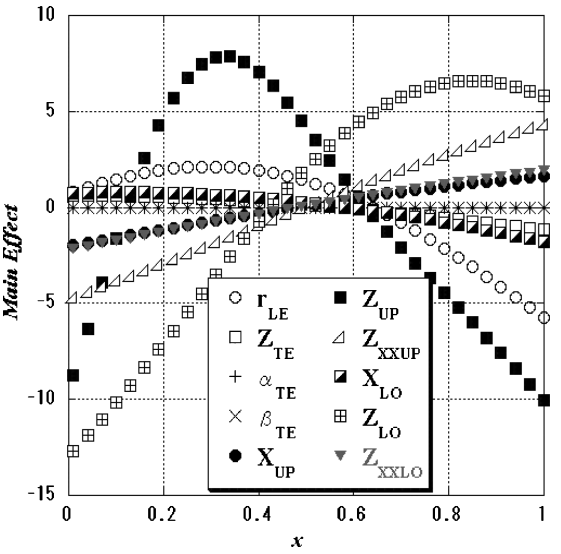

Fig. 9 Main effect of design variables.

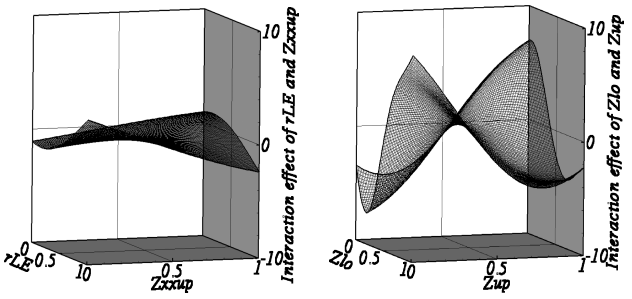

a) b)

Fig. 10 Design variables two-way interactions: a) between r_{LE} and Z_{XXup} and b) between Z_{lo} and Z_{up}.

main effect of the design variables. According to the shown main effect, the objective function, L/D, is sensitive to the change of Z_{lo}, Z_{up}, r_{LE}, Z_{XXup}, and Z_{XXlo} and is insensitive to the change of other design variables. There are 45 two-way interactions because the number of design variables is 10. Two of those two-way interactions are plotted in Fig. 10. According to the result, the objective function is sensitive to the change of the interaction Z_{up}–Z_{lo} and is insensitive to the change of the interaction r_{LE}–Z_{XXup}.

The proportion of the variance due to each design variable and their interactions to the total variance was calculated by using Eq. (19). Design variables and their interactions whose proportion to total variance is over than 1.0% are shown in Fig. 11. According to these results, it seems that Z_{lo}, Z_{up}, r_{LE}, Z_{XXup}, and Z_{XXlo} are very important variables in L/D optimization design. On the other hand, other parameters seem less important to the design of high L/D airfoil.

Design of Airfoil Using Five Variables

To verify the result of the functional ANOVA, airfoil design was performed with only five important design variables, Z_{lo}, Z_{up}, r_{LE}, Z_{XXup}, and Z_{XXlo}. The geometry and pressure distribution of the optimized airfoil with 5 design variables are compared with those of the optimized airfoil with 10 design variables and RAE2822 in Fig. 12. The geometry near the trailing edge shows a somewhat large

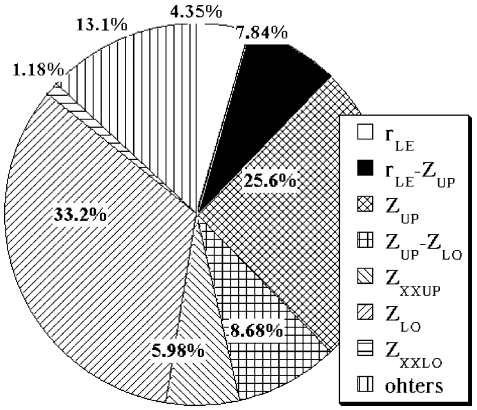

Fig. 11 Proportion to the total variance.

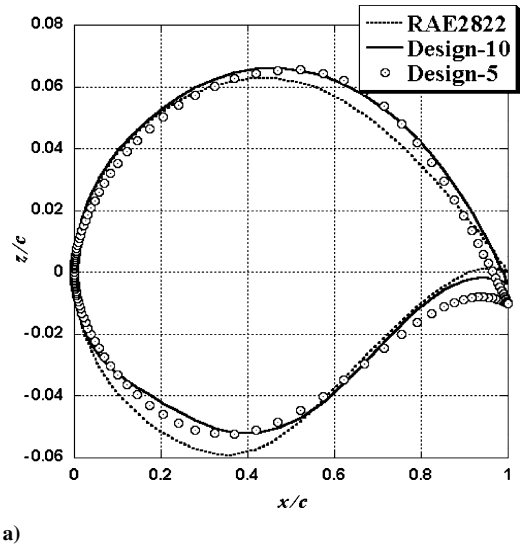

a)

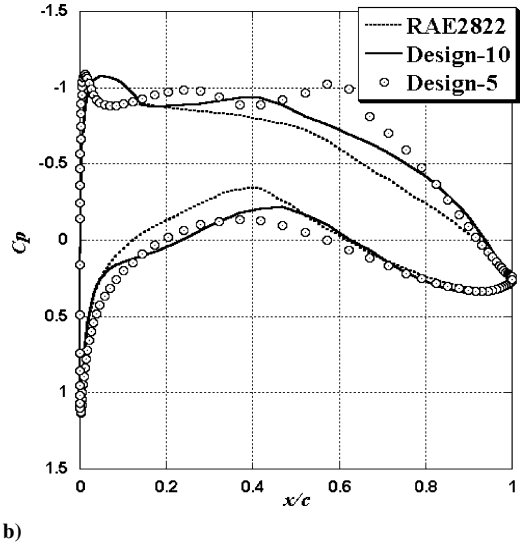

b)

Fig. 12 Airfoils comparisons of a) geometry and b) pressure distribution.

difference between the design results of 5-variable and 10-variable cases because the design variables defining the shape near the trailing edge are fixed in the 5-variable case. The L/D performance and cross-sectional area of the airfoil designed with 5 variables are also compared with those of the airfoil designed with 10 variables and RAE2822 in Table 3. The L/D of the 5-variable case is slightly lower than that of the 10-variable case; however, it is still larger than that of RAE2822, while satisfying the design constraint. It shows

Table 3 Comparison of *L/D* and cross-sectional area of airfoils

Airfoil	L/D	Area of cross section
RAE2822	58.0178	7.7777*e*-02
Design-10	60.7546	7.8637*e*-02
Design-5	60.1225	7.7997*e*-02

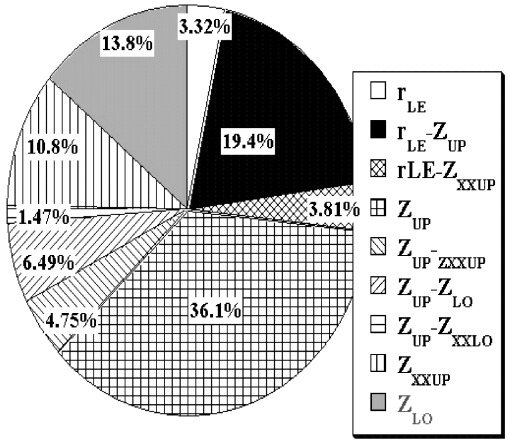

Fig. 13 Proportion to total variance.

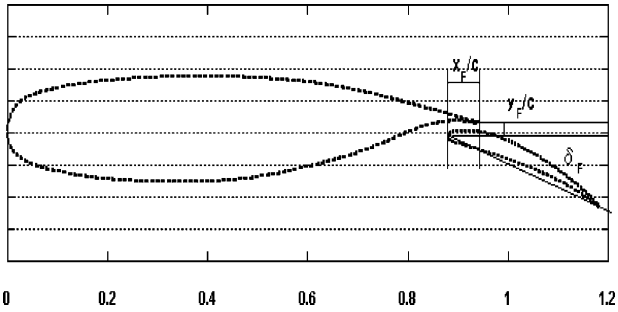

Fig. 14 NLR7301 with single flap.

the validity of the eliminating the design variable that has little influence on the objective function based on the result of the functional ANOVA. For the case of five design variables, the functional ANOVA was also performed. Figure 13 shows the proportion of variance due to the each design variable and their interactions to the total variance of model. According to the result, Z_{up}, r_{LE}–Z_{up}, Z_{lo}, and $Z_{XX\text{up}}$ have a large influence on L/D.

Optimization of Flap's Position

The second optimization problem is to find the position of the flap where the L/D of multi-element airfoil is maximized at a specified flow condition: Mach $= 0.185$, AOA $= 6$ deg, and $Re = 2.51 \times 10^6$.

Geometry and Design Space

The multi-elements airfoil used in the study is the National Aerospace Laboratory NLR7301[15] with single flap of 32% chord. The position of flap is defined by three parameters, x_F/c, y_F/c, and δ_F, as shown in Fig. 14. The parameter ranges of design space are defined as follows:

$$-5 \le x_F/c \le 10\% \tag{22}$$

$$2 \le y_F/c \le 10\% \tag{23}$$

$$0 \le \delta_F \le 40 \text{ deg} \tag{24}$$

Selection of Sample Points and Evaluation

By the use of OAs of strength 5 and level 2, 25 sample points were selected. The evaluations of sample points are performed using Tohoku University Aerodynamic Simulation (TAS) code that

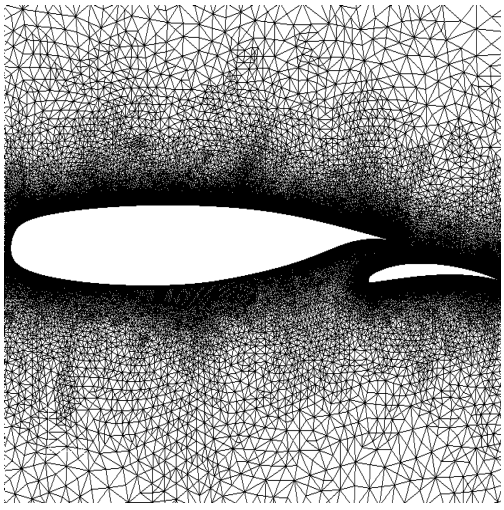

a)

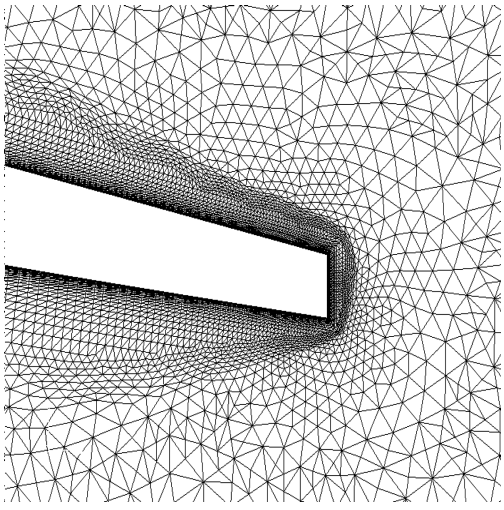

b)

Fig. 15 Unstructured mesh around the multi elements airfoil: a) overview of computational mesh and b) prism layer near the wall.

is composed of unstructured mesh generator (TAS_MESH)[16,17] and flow solver (TAS_FLOW). Figure 15 shows the computational mesh around the multi-element airfoil generated by TAS_MESH. The prisms' layers are located near the wall for the viscous flows.

The flow solver, TAS_FLOW, is a Navier–Stokes code that uses a finite volume cell-vertex scheme. The Haren–Lax–van Leer–Einfeldt–Wada Riemann solver (HLLEW) is used for the numerical flux calculation, and the LU_SGS method is used for time integration. The Spalart–Allmaras model[18] is implemented to treat the turbulent layer.

GA with Kriging Model

The performance of 25 sample points was evaluated using TAS code, and then the kriging model was constructed based on these sample data. The kriging model was utilized for the objective function evaluation in the process of GA. Instead of searching for the maximum L/D point on the kriging model directly, GA searches for the maximum EI point on the kriging model to improve the robustness in finding the global optimum point. The predicted optimum position of flap is $x_F/c = 1.82\%$, $y_F/c = 5.78\%$, and $\delta_F = 9.66$ deg, and the L/D at that position was 85.47. Figure 16 shows the L/D (at $\delta_F = 9.66$ deg) predicted by the kriging model. According to Fig. 16, the L/D of the multi-element airfoil, NLR7301, is very sensitive to the y_F/c, whereas it is insensitive to x_F/c. L/D increases steadily as y_F/c approaches 10% because the interference

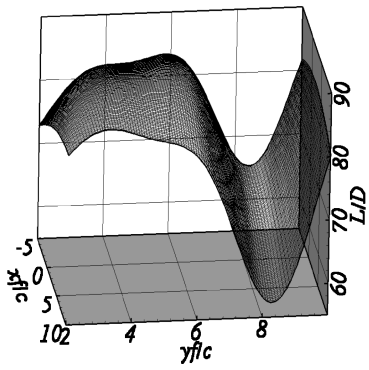

Fig. 16 Kriging surface of *L/D* at deflection angle $\delta_F = 9.66$ deg.

between main airfoil and flap weaken. In this condition, L/D of the main airfoil is almost constant, and L/D of the flap slightly increases. Thus, the total L/D increases. If y_F/c becomes larger than a certain value, the interference completely disappears, and the total L/D becomes constant. L/D at that position may be larger than the predicted L/D, but from the structural point of view, y_F/c of 10% or greater is difficult to realize. Thus, the maximum L/D position is searched within the range of $y_F/c < 10\%$ in this study.

Conclusions

In this study, the GA using the kriging model for objective function evaluation was introduced. The kriging model is a response surface model that represents a relationship between the objective function (output) and design variables (input) using a stochastic process. Replacing the CFD solver with the kriging model drastically reduced the computational time required for the objective function evaluation. A criterion known as EI was used for the selection of additional sample points. This enables us not only to improve the accuracy of the response surface but also to explore the global optimum efficiently. The functional ANOVA was conducted to evaluate the effect of each design variable and its interactions to the objective function. This was very helpful in reducing the number of design variables. The present method was applied to a two-dimensional airfoil design and the prediction of a flap's position where the L/D of a two-element airfoil is maximized. The result confirmed the validity of the present method.

References

[1]Myers, R. H., and Montgomery, D. C., *Response Surface Methodology: Process and Product Optimization Using Designed Experiments*, Wiley, New York, 1995, pp. 1–84.

[2]Chen, W., Allen, J. K., Schrage, D. P., and Mistree, F., "Statistical Experimentation Methods for Achieving Affordable Concurrent Systems Design," *AIAA Journal*, Vol. 35, No. 5, 1997, pp. 892–900.

[3]Timothy, W. S., Timothy M. M., John, J. K., and Farrokh, M., "Comparison of Response Surface and Kriging Models for Multidisciplinary Design Optimization," AIAA Paper 98-4755, Sept. 1998.

[4]Anthony, A. G., and Layne, T. W., "A Comparison of Approximation Modeling Techniques: Polynomial Versus Interpolating Models," AIAA Paper 98-4758, Sept. 1998.

[5]Sack, J., Welch, W. J., Mitchell, T. J., and Wynn, H. P., "Design and Analysis of Computer Experiments (with Discussion)," *Statistical Science*, Vol. 4, 1989, pp. 409–435.

[6]Booker, A. J., "Design and Analysis of Computer Experiments," AIAA Paper 98-4757, Sept. 1998.

[7]Koehler, J., and Owen, A., "Computer Experiments," *Handbook of Statistics, 13*: *Design and Analysis of Experiments*, edited by S. Ghosh and C. R. Rao, Elsevier, Amsterdam, 1996, pp. 261–308.

[8]Mardia, K. V., and Marshall, R. J., "Maximum Likelihood Estimation of Models for Residual Covariance in Spatial Regression," *Biometrika*, Vol. 71, 1984, pp. 135–146.

[9]Goldberg, D. E., *Genetic Algorithms in Search, Optimization & Machine Learning*, Addison Wesley Longman, Reading, MA, 1989.

[10]Takami, H., Kita, H., and Kobayashi, S., "Multi-Objective Optimization by Genetic Algorithms: A Review," *Proceedings of 1996 IEEE International Conference on Evolutionary Computation*, IEEE Publications, Piscataway, NJ, 1996, pp. 517–522.

[11]Donald, R. J., Matthias, S., and William, J. W., "Efficient Global Optimization of Expensive Black-Box Function," *Journal of Global Optimization*, Vol. 13, 1998, pp. 455–492.

[12]Sobieczky, H., "Parametric Airfoils and Wings," *Recent Development of Aerodynamic Design Methodologies—Inverse Design and Optimization*, Friedr. Vieweg & Sohn Verlagsgesellschaft mbH, Brunswick, Germany, 1999, pp. 71–87.

[13]Owen, A. B., "Orthogonal Arrays for Computer Experiments, Integration and Visualization," *Statistica Sinica*, Vol. 2, 1992, pp. 439–452.

[14]Obayashi, S., and Guruswamy, G. P., "Convergence Acceleration of an Aeroelastic Navier–Stokes Solver," *AIAA Journal*, Vol. 33, No. 6, 1995, pp. 1134–1141.

[15]Van der Berg, B., "Boundary Layer Measurements on a Two-Dimensional Wing with Flap," National Aerospace Lab., NLR TR 79009 U, The Netherlands, 1979.

[16]Sharov, D., and Nakahashi, K., "A Boundary Recovery Algorithm for Delaunay Tetrahedral Meshing," *Proceedings of 5th International Conference on Numerical Grid Generation on Computational Field Simulations*, 1996, pp. 229–238.

[17]Ito, Y., and Nakahashi, K., "Unstructured Mesh Generation for Viscous Flow Computations," *Proceedings of the 11th International Meshing Roundtable*, 2002, pp. 367–376.

[18]Fares, E., Meinke, M., and Schder, W., "Numerical Engine Jets in the Near Field," AIAA Paper 2000-2222, Jan. 2000.